Mechano-chemical feedback leads to cell competition for cell fate specification

Daniel, J. Toddie-Moore[1¶*], Martin, P. Montanari[1], Isaac Salazar-Ciudad[1,2,3] and Osamu Shimmi[1,4*]

[1]Institute of Biotechnology, University of Helsinki, 00014 Helsinki, Finland

[2]Genomics, Bioinformatics and Evolution. Departament de Genètica i Microbiologia, Universitat Autònoma de Barcelona, 08193, Cerdanyola del Vallès, Spain

[3]Centre de Rercerca Matemàtica, 08193, Cerdanyola del Vallès, Spain

[4]Institute of Molecular and Cell Biology, University of Tartu, 51010 Tartu, Estonia

[*]Corresponding authors:

d.toddie-moore@ed.ac.uk and osamu.shimmi@helsinki.fi

[¶]Present address: University of Edinburg, United Kingdom

Abstract

Developmental patterning is thought to be regulated by conserved signalling pathways. Initial patterns are often broad before refining to only those cells that commit to a particular fate[1,2]. However, the mechanisms by which pattern refinement takes place remain to be addressed. Using the posterior crossvein (PCV) of the *Drosophila* pupal wing as a model, into which bone morphogenetic protein (BMP) ligand is extracellularly transported to instruct vein patterning[3,4], we investigate how pattern refinement is regulated. We found that BMP signalling induces apical enrichment of Myosin II in developing crossvein cells to regulate apical constriction. Live imaging of cellular behaviour indicates that changes in cell shape are dynamic and transient, only being maintained in those cells that retain vein fate after refinement. Disrupting cell shape changes throughout the PCV inhibits pattern refinement. In contrast, disrupting cell shape in only a subset of vein cells can result in a loss of BMP signalling. We propose that cell shape changes of future PCV cells allow them to compete more efficiently for basally localised BMP signal by forming a mechano-chemical feedback loop. This study highlights a new form of cell competition: competing for a signal that induces cell fate rather than promotes cell survival.

Main

Pattern formation is a fundamental process in animal development, for which various molecular mechanisms have been proposed, including gene regulatory networks and growth factor signalling[1,2]. Developmental patterning often involves refinement from a broad initial area of competency for a fate to only those cells that commit to it, with neighbours losing competence and following an alternate fate path (Fig. 1a)[1,2]. Whilst some mechanisms of pattern refinement, such as transcriptional networks and lateral inhibition, have previously been investigated, the role played by diffusible growth factor signalling, in particular the interactions between signalling and morphogenesis, has been less explored[5,6].

The PCV of the *Drosophila* pupal wing serves as an excellent model to address the dynamics of signalling and morphogenesis, as its formation is initially directed by a single signalling pathway: BMP signalling[4,7]. The *Drosophila* BMP ligand Decapentaplegic (Dpp) is initially expressed in the adjacent longitudinal veins (LVs) and is extracellularly transported into the prospective PCV region along the basal surfaces of the two cell layers that comprise the wing epithelia (Fig. 1b)[3]. BMP signalling induced by the Dpp ligand forms the PCV field by becoming competent for vein, rather than intervein fate (Fig. 1c). Continuous extracellular Dpp transport seems to be crucial for a period of around 10 hours (18 – 28 h after pupariation (AP)) to maintain the PCV field and vein fate competence, before PCV cells begin to express the ligand themselves[7]. Continued extracellular signalling and vein morphogenesis occur concurrently, as morphogenesis begins shortly after BMP signalling is activated[4]. Refinement of the BMP signalling pattern during this time window has previously been observed; however how pattern refinement takes place has not been addressed[8].

BMP signal induces cell shape changes

First, we confirmed that refinement of the PCV field takes place during morphogenesis. The PCV field is defined as the cells in which BMP signalling occurs, as indicated by staining with anti-phosphorylated Mad antibody (pMad)[9], and which are therefore competent to assume a vein fate. Our data reveal that the number of cells within the PCV field reduces between 20h AP, shortly after the initiation of PCV patterning, and 28h AP, when PCV cells express *dpp* themselves (Fig. 1d, e). Thus we term the period from 20 to 28 hours AP the ‘refinement period’.

During this period, apical constriction of vein cells appears to be the hallmark of vein morphogenesis[8,10]. Since BMP signalling is thought to initiate PCV development[3], we next asked whether BMP signalling directs the wing vein-like cell shape changes (thereafter referring as “cell shape changes") that occur during PCV morphogenesis. To answer this question, we captured images of apical cell shapes in *crossveinless* mutant wings, where BMP signalling is inactive in the PCV region, and observed that apical constriction does not occur (Fig. 1f)[11]. These results indicate that BMP signalling is required for the cell shape changes that occur during PCV morphogenesis.

The activity of Myosin II (MyoII) has been proposed to be the driving force behind cell shape dynamics such as apical constriction[12]. To investigate whether BMP signalling directs cell shape change through MyoII activity, we analysed the spatial localisation of MyoII using MyoII regulatory light chain (MRLC) tagged with RFP in wild type and *crossveinless* pupal wings[13]. In wildtype wings, MyoII is enriched in the apical compartment of PCV cells, with lower basal levels, but in contrast, neighbouring intervein cells have lower apical levels of MyoII than the PCV (Fig. 1g, Extended Data Fig. 1a). Conversely, in *crossveinless* pupal wings, apical MyoII enrichment is not observed in the PCV region, although apical enrichment of MyoII is still detected in LVs (Fig. 1g, Extended Data Fig. 1a). These findings suggest that BMP signalling facilitates the apical localisation of MyoII to promote apical constriction of PCV cells. This was further confirmed by the observation that ectopic expression of the constitutively active form of BMP type I receptor in mosaic analysis with a repressible cell marker (MARCM) clones within the pupal wing induces apical enrichment of MyoII, as well as strong apical constriction (Extended Data Fig. 1b)[8,14].

Time lapse imaging during vein morphogenesis

As wing vein morphogenesis directed by BMP signalling and refinement of the BMP signalling pattern occur concurrently, we hypothesised that these events could be mutually coordinated. To address this, we employed *in vivo* live imaging of pupal wings expressing GFP tagged E-cadherin to observe cell shape changes during the refinement period[15]. We tracked the apical shapes of cells that are part of the PCV at the end of the refinement period, and thus retained vein fate, and compared it to the cells flanking this region (Fig. 2a-c, Supplementary Videos 1-3). Intriguingly, whilst the cells which will form the PCV apically constrict throughout the refinement period, several of the cells immediately flanking these constrict apically at early time points but fail to maintain their vein-like morphology at later time points, eventually reverting to an intervein fate (Fig. 2a-c, Supplementary Videos 1, 2).

Cell shape change and pattern refinement

We hypothesised that cell shape changes themselves may affect signalling pattern refinement and thus cell fate choice in the PCV region (Fig. 2d). To test this idea, we modulated cell shape changes in the developing wing by attenuating MyoII activity using a dominant negative form of the Myosin Heavy Chain (MyoII-DN)[16]. Inhibiting MyoII activity across the posterior wing blade for 10 hours during PCV morphogenesis is sufficient to disrupt apical constriction in the PCV region and LV cells of 25h AP pupal wings (Extended Data Fig. 2a). Intriguingly, loss of MyoII activity throughout posterior wing results in a broader range of BMP signalling in the PCV region than in control wings, suggesting that cell shape changes are necessary for the refinement of the BMP signalling but not for BMP signalling itself (Fig. 3a, b). Additionally BMP signalling is missing in the PCV region when MyoII activity was disrupted in the posterior half of wings of *crossveinless* background, indicating that the unrefined BMP signalling pattern is still being directed by extracellular BMP signalling (Extended Data Fig 2b).

What then is the role of cell shape changes in signalling pattern refinement? Despite reversal of BMP-induced cell shape changes being associated with reduced competence for vein fate, blocking cell shape changes did not affect BMP signalling. We hypothesised that what might be important is not cell shape change itself, but how cell morphology compares to that of other cells within the field. The impact of cell shape change loss may then be context specific, facilitating refinement by causing less signalling and fate loss in cells surrounded by those with greater changes in shape. If this the case, inhibition of cell shape changes in a small group of cells within the PCV field may decrease their ability to retain BMP signalling and vein fate. We tested this hypothesis by generating clones that attenuate cell shape changes amongst neighbours that are wild type. Strikingly, when MyoII attenuated clones are produced within the PCV field, loss of BMP signalling can often be observed in context dependent manner (Fig. 3c, Extended Data Fig. 2c). This suggests that MyoII-based cell shape changes play a crucial role in whether a cell retains vein fate during refinement, despite not being required for competency for BMP signalling. When all PCV field cells cannot form vein-like shapes, signalling still occurs throughout and refinement does not take place (Fig. 3a, b, d, Extended Data Fig. 4b). However, when cells are present in a heterogeneous population with or without cell shape changes, cells that can change shape both retain the signal and acquire vein fate (Fig. 3c, d, Extended Data Fig. 4b). We propose that this represents a novel type of cell competition; where the outcome instructs cell fate determination rather than survival or elimination (Fig. 2d, Extended Data Fig. 4a, b). Winner cells are those within the field that retain cell shape changes and acquire vein fate by maintaining BMP signalling, whereas loser cells are less competitive for the BMP signal, resulting in the inability to retain shape, and revert to intervein fate (Extended Data Fig. 4). Furthermore, our data indicate that the mechanism of pattern refinement is a mechano-chemical feedback loop as BMP signalling induces the cell shape changes, which in turn influence the ability of cells to retain that signal.

Basal cell shape and cell competition

We next considered what the mechanism of cell shape change-mediated cell competition could be. Previous studies indicate that extracellularly trafficked Dpp ligands are predominantly localised on the basal side of the wing epithelia[3]. Since BMP receptor appears to be down-regulated by BMP signalling throughout wing development, expression of receptors may not explain the mechanism[3,17]. Thus, we hypothesized that expansion in basal cell size may increase competitiveness for capturing basal ligand within the signalling microenvironment, resulting in producing winner cells. We therefore investigated the basal size dynamics of PCV field cells[3]. We observed that cells at the periphery of the PCV field (that lose their fate during refinement) are consistently smaller than those at the centre of the field during the refinement period (Fig. 4a, b).

To examine whether differential basal cell size is a mechanism by which cell competition for cell fate could occur, we observed whether differences in basal cell size within the PCV field are still observed when refinement does not take place due to attenuated MyoII activity. We observed that unlike wild type wings differences in basal cell surface between central and peripheral cells are not observed when MyoII activity is disrupted in the posterior half of pupal wing (Extended Data Fig 3a). These data are consistent with basal cell size dynamics playing a role in the mechanism of cell competition-mediated refinement.

Furthermore, we found that the basal surfaces of *crossveinless* cells do not expand in the region between L4 and L5 where the PCV field should form, suggesting that BMP signalling plays a positive role in the basal expansion of these cells (Extended Data Fig. 3b). Considering that BMP signalling induces apical but not basal enrichment of MyoII in the PCV region (Fig. 1g, Extended Data Fig. 1a), it is likely that BMP induced apical constriction is important for changes in basal shape and forms a mechano-chemical feedback loop facilitating cell competition for cell fate, which lead to pattern refinement.

Discussion

Here we found that cell shape changes are coupled to the refinement of BMP signalling during PCV morphogenesis. Our findings reveal that cell shape changes drive refinement by directing competition for the vein fate-determining BMP ligand, with loser cells acquiring intervein cell fate. Previous studies have proposed that competition between cells for BMP signalling instructs the pattern of survival and elimination in the *Drosophila* wing imaginal disc[18-20]. Since BMP signalling is one of the key players regulating cell proliferation in the larval wing imaginal disc[21,22], cells lacking BMP signalling are less proliferative than neighbouring cells and are eliminated as loser cells (Extended Data Fig. 4)[23]. Although BMP still serves as a proliferative signal in the *Drosophila* wing during the early pupal stage[24,25], BMP turns into a cell differentiation factor at the beginning of the refinement period and thus competition has a different outcome. Therefore, competition for the BMP signal leads to winner and loser cells acquiring different cell fates (vein or intervein) in later pupal development (Extended Data Fig. 4).

Our data suggest that dynamic basal cell shape changes are important for the determination of winner and loser cells and may allow PCV field cells to better compete for extracellular ligand or space within the signalling micro-environment. Although BMP signalling is needed for cell shape changes to occur, the differences in basal cell dynamics within the PCV field may not be directly regulated by BMP signalling. Although previous studies have shown that BMP signalling induces the expression of several molecules in the PCV region to optimize the BMP signalling by forming a feedback loop[4,8,26], the expression of these factors begins from the early refinement stage and thus initial differential transcription is unlikely to instruct differences in basal shape dynamics. They may instead play a role in amplifying differences in the levels of BMP signalling between winner cells and loser cells during refinement.

Changes in the 3D architecture of the pupal wing epithelia, such as apposition of the two wing layers, are also unlikely to be responsible for differences in basal cell size. Unlike our recent observations that the 3D architecture of pupal wing epithelia and BMP signalling in the LVs are coupled[24], PCV refinement appears to be a 2D phenomenon as large single layer clones expressing MyoII-DN that disrupt 3D architecture have been observed which do not affect refinement in the other layer (Extended Data Fig. 2d). We rather consider that a cellular mechanical network within the PCV field may trigger the differences in basal dynamics[5,6,27,28], therefore we propose that the formation of differential basal dynamics during refinement is a self-organising process[2]. Further study is needed to fully understand how basal cell shape dynamics are regulated during cell competition.

We suspect that cell competition for cell fate is likely to be a general mechanism for self-organisation of pattern refinement during development. Cell shape changes are a common part of the morphogenesis programme and could feed back into developmental patterning in a variety of contexts[5,6]. Apical constriction and basal expansion are an important aspect of epithelial folding, a process which has broadly been linked to cell fate decisions and developmental patterning[5,6,29,30]. Our finding that cell shape changes within the 2D epithelial layer, irrespective of epithelial folding, can instruct pattern refinement provides a novel insight into epithelial morphogenesis.

In summary, our data reveal that cell shape changes influence refinement of the signalling pattern by facilitating cell competition for signalling pathway activation. We have uncovered that cell competition occurs via a mechano-chemical feedback loop between cell shape changes and BMP signalling, leading to self-organising refinement of the developmental field during pattern formation.

Acknowledgements

We are grateful to Jukka Jernvall and Yukitaka Ishimoto for thoughtful comments on the manuscript. We thank Light microscopy Unit, University of Helsinki for their support. We thank H. Ohkura, R. Le Borgne, D. Kiehart and A. Martin for fly stocks. This work was supported by grant 308045 from the Academy of Finland, the Sigrid Juselius Foundation to O.S., grant 295013 from the Academy of Finland to D.T-M., and the Center of Excellence in Experimental and Computational Developmental Biology from the Academy of Finland to O.S. and I.S-C.

Author contributions

D.T-M. and O.S. conceived the project and planned experiments. D.T-M. and M.M. performed all experiments. D.T-M. analysed the results and discussed them with O.S. I.S-C. provided inputs. D.T-M. and O.S. wrote the manuscript and all authors made comments. O.S. supervised the project.

Declaration of interests

The authors declare no competing interest.

Data availability

Source Data for Figs. 1e, 2b, 3b, 4b are provided with the paper.

References

1 Morelli, L. G., Uriu, K., Ares, S. & Oates, A. C. Computational approaches to developmental patterning. *Science* **336**, 187-191, doi:10.1126/science.1215478 (2012).

2 Schweisguth, F. & Corson, F. Self-Organization in Pattern Formation. *Dev Cell* **49**, 659-677, doi:10.1016/j.devcel.2019.05.019 (2019).

3 Matsuda, S. & Shimmi, O. Directional transport and active retention of Dpp/BMP create wing vein patterns in Drosophila. *Dev Biol* **366**, 153-162, doi:10.1016/j.ydbio.2012.04.009 (2012).

4 Matsuda, S., Blanco, J. & Shimmi, O. A feed-forward loop coupling extracellular BMP transport and morphogenesis in Drosophila wing. *PLoS Genet* **9**, e1003403, doi:10.1371/journal.pgen.1003403 (2013).

5 Hannezo, E. & Heisenberg, C. P. Mechanochemical Feedback Loops in Development and Disease. *Cell* **178**, 12-25, doi:10.1016/j.cell.2019.05.052 (2019).

6 Gilmour, D., Rembold, M. & Leptin, M. From morphogen to morphogenesis and back. *Nature* **541**, 311-320, doi:10.1038/nature21348 (2017).

7 Ralston, A. & Blair, S. S. Long-range Dpp signaling is regulated to restrict BMP signaling to a crossvein competent zone. *Dev Biol* **280**, 187-200, doi:10.1016/j.ydbio.2005.01.018 (2005).

8 Gui, J., Huang, Y. & Shimmi, O. Scribbled optimizes BMP signaling through its receptor internalization to the Rab5 endosome and promote robust epithelial morphogenesis. *PLoS Genet* (2016).

9 Ross, J. J. *et al.* Twisted gastrulation is a conserved extracellular BMP antagonist. *Nature* **410**, 479-483, doi:10.1038/35068578 (2001).

10 Fristrom, D., Wilcox, M. & Fristrom, J. The distribution of PS integrins, laminin A and F-actin during key stages in Drosophila wing development. *Development* **117**, 509-523 (1993).

11 Shimmi, O., Ralston, A., Blair, S. S. & O'Connor, M. B. The crossveinless gene encodes a new member of the Twisted gastrulation family of BMP-binding proteins which, with Short gastrulation, promotes BMP signaling in the crossveins of the Drosophila wing. *Dev Biol* **282**, 70-83, doi:10.1016/j.ydbio.2005.02.029 (2005).

12 Martin, A. C. & Goldstein, B. Apical constriction: themes and variations on a cellular mechanism driving morphogenesis. *Development* **141**, 1987-1998, doi:10.1242/dev.102228 (2014).

13 Daniel, E. *et al.* Coordination of Septate Junctions Assembly and Completion of Cytokinesis in Proliferative Epithelial Tissues. *Curr Biol* **28**, 1380-1391 e1384, doi:10.1016/j.cub.2018.03.034 (2018).

14 Lee, T. & Luo, L. Mosaic analysis with a repressible cell marker for studies of gene function in neuronal morphogenesis. *Neuron* **22**, 451-461 (1999).

15 Shimada, Y., Yonemura, S., Ohkura, H., Strutt, D. & Uemura, T. Polarized transport of Frizzled along the planar microtubule arrays in Drosophila wing epithelium. *Dev Cell* **10**, 209-222, doi:10.1016/j.devcel.2005.11.016 (2006).

16 Franke, J. D., Montague, R. A. & Kiehart, D. P. Nonmuscle myosin II generates forces that transmit tension and drive contraction in multiple tissues during dorsal closure. *Curr Biol* **15**, 2208-2221, doi:10.1016/j.cub.2005.11.064 (2005).

17 de Celis, J. F. Expression and function of decapentaplegic and thick veins during the differentiation of the veins in the Drosophila wing. *Development* **124**, 1007-1018 (1997).

18 Moreno, E., Basler, K. & Morata, G. Cells compete for decapentaplegic survival factor to prevent apoptosis in Drosophila wing development. *Nature* **416**, 755-759, doi:10.1038/416755a (2002).

19 Moreno, E. & Basler, K. dMyc transforms cells into super-competitors. *Cell* **117**, 117-129, doi:10.1016/s0092-8674(04)00262-4 (2004).

20 Adachi-Yamada, T. & O'Connor, M. B. Morphogenetic apoptosis: a mechanism for correcting discontinuities in morphogen gradients. *Dev Biol* **251**, 74-90 (2002).

21 Affolter, M. & Basler, K. The Decapentaplegic morphogen gradient: from pattern formation to growth regulation. *Nat Rev Genet* **8**, 663-674, doi:10.1038/nrg2166 (2007).

22 Restrepo, S., Zartman, J. J. & Basler, K. Coordination of patterning and growth by the morphogen DPP. *Curr Biol* **24**, R245-255, doi:10.1016/j.cub.2014.01.055 (2014).

23 Bowling, S., Lawlor, K. & Rodriguez, T. A. Cell competition: the winners and losers of fitness selection. *Development* **146**, doi:10.1242/dev.167486 (2019).

24 Gui, J. *et al.* Coupling between dynamic 3D tissue architecture and BMP morphogen signaling during Drosophila wing morphogenesis. *Proc Natl Acad Sci U S A*, doi:10.1073/pnas.1815427116 (2019).

25 Milan, M., Campuzano, S. & Garcia-Bellido, A. Cell cycling and patterned cell proliferation in the Drosophila wing during metamorphosis. *Proc Natl Acad Sci U S A* **93**, 11687-11692 (1996).

26 Serpe, M. *et al.* The BMP-binding protein Crossveinless 2 is a short-range, concentration-dependent, biphasic modulator of BMP signaling in Drosophila. *Dev Cell* **14**, 940-953, doi:10.1016/j.devcel.2008.03.023 (2008).

27 Pinheiro, D. & Bellaiotache, Y. Mechanical Force-Driven Adherens Junction Remodeling and Epithelial Dynamics. *Dev Cell* **47**, 391, doi:10.1016/j.devcel.2018.10.021 (2018).

28 Irvine, K. D. & Shraiman, B. I. Mechanical control of growth: ideas, facts and challenges. *Development* **144**, 4238-4248, doi:10.1242/dev.151902 (2017).

29 Sivakumar, A. & Kurpios, N. A. Transcriptional regulation of cell shape during organ morphogenesis. *J Cell Biol* **217**, 2987-3005, doi:10.1083/jcb.201612115 (2018).

30 Heer, N. C. & Martin, A. C. Tension, contraction and tissue morphogenesis. *Development* **144**, 4249-4260, doi:10.1242/dev.151282 (2017).

31 Rauzi, M., Lenne, P. F. & Lecuit, T. Planar polarized actomyosin contractile flows control epithelial junction remodelling. *Nature* **468**, 1110-1114, doi:10.1038/nature09566 (2010).

32 Buttitta, L. A., Katzaroff, A. J., Perez, C. L., de la Cruz, A. & Edgar, B. A. A double-assurance mechanism controls cell cycle exit upon terminal differentiation in Drosophila. *Dev Cell* **12**, 631-643, doi:10.1016/j.devcel.2007.02.020 (2007).

33 Ashburner, M., Golic, K. G. & Hawley, R. S. Drosophila: A Laboratory Handbook, Second Edition (Cold Sprig Habor, NY: Cold Spring Habor Press). (2004).

34 Amoyel, M. & Bach, E. A. Cell competition: how to eliminate your neighbours. *Development* **141**, 988-1000, doi:10.1242/dev.079129 (2014).

Materials and methods

Fly genetics

UAS-mCD8::GFP (#5137) and *en-Gal4* (#30564) were obtained from the Bloomington *Drosophila* Stock Centre. *UAS-tkv*^{Q253D} and *cv*^{70} were described previously[8,11]. *Shg::GFP* was obtained from H. Ohkura[15], *MyoII::RFP* from R. Le Borgne[13], *UAS-MyoII-DN* from D. Kiehart[16] and *sqh-GAP43::mCherry* from A. Martin[31]. Flies were raised at 25°C unless otherwise stated. Populations of mixed sex were used except for when using *yw*, where females were selected, and experiments involving *crossveinless* where only males were used. The age of pupal wingsat dissection are given at developmental timepoints equivalent to 25 ºC. Calculations for relative developmental timing at 18 ºC, 25 ºC and 29 ºC were based on previously published data and rounded to the nearest hour[32,33]. For experiments using *en-Gal4* pupae were raised at 18°C for 22 hours after pupariation, and then shifted to 29°C for either 10 (Fig. 3a, Extended Data Fig. 2a, b) or 12 (Extended Data Fig. 3a) hours before dissection and fixation. For clone generation larvae were raised at 25°C for 3-4 days AEL (or 18°C for 6-7 days AEL), before being heat shocked in a 37°C water bath for 1 hour. Vials containing larvae were then placed in 18°C until at the white pre-pupal stage when they were transferred to 29°C for 21 hours before dissection and fixation. For time lapse imaging pupae were raised at 25°C until 17 hours after the pre-pupal stage. They were then moved to room temperature for one hour during which time windows were cut into the pupal case and pupae mounted before being imaged as previously described[24].

Full genotypes

Fig. 1d, 4a,: *yw*

Fig. 1f and Extended Data Fig. 3b: *yw; ubi-shg::GFP,* or *cv*^{70}*; ubi-shg::GFP*

Fig. 1g and Extended Data Fig. 1a: *MyoII::RFP,* or *MyoII::RFP, cv*^{70}

Fig. 2a and Suppl videos 1-3: *ubi-shg::GFP/sqh-Gap43::mCherry*

Fig. 3a and Extended Data Fig. 2a: *en-Gal4/UAS-mCD8::GFP; tubP-Gal80*^{ts}*,* or *en-Gal4/UAS-MyoII-DN; tubP-Gal80*^{ts}

Fig. 3c and Extended Data Fig. 2c and d: *hs-Flp; tubP-Gal4 UAS-mCD8::GFP/UAS-MyoII-DN; tubP-Gal80 FRT*^{82B} */FRT*^{82B}

Extended Data Fig. 1b: *hs-Flp/tubP-Gal80*^{ts}*, MyoII::RFP; tubP-Gal4 UAS-mCD8::GFP/UAS-tkv*^{Q253D} *(caTKV); tubP-Gal80 FRT*^{82B} */FRT*^{82B}

Extended Data Fig. 2b: *cv*^{70}*; en-Gal4/+; tubP-Gal80*^{ts}, or *cv*^{70}*;en-Gal4/UAS-MyoII-DN; tubP-Gal80*^{ts}

Extended Data Fig. 3a: *en-Gal4/sqh-Gap43::mCherry; tubP-Gal80*^{ts}, or *en-Gal4/UAS-MyoII-DN, sqh-Gap43::mCherry; tubP-Gal80*^{ts}

Immunohistochemistry

Pupae were fixed in 3.7% formaldehyde (Sigma-Aldrich) for 2 nights at 4°C before dissecting the pupal wings, removing the cuticle and blocking with Normal Goat Serum (10%) overnight. Both primary and secondary antibody incubations also took place overnight at 4°C. The following primary antibodies were used: mouse anti-DLG1 [1:40; Developmental Studies Hybridoma Bank (DSHB), University of Iowa] and rabbit anti-phospho-SMAD1/5 (1:200; Cell Signaling Technologies). Secondary antibodies were anti-rabbit IgG Alexa 568 (1:200, Invitrogen), anti-mouse IgG Alexa 647 (1:200; Life technologies), anti-rabbit IgG Alexa 647 (1:200; Life technologies). F-actin was stained with Alexa 488 conjugated phalloidin (1:200; Life technologies).

Imaging and Image Analysis

Confocal images and time lapse imaging was conducted using a Leica SP8 STED confocal microscope. Time lapse images were processed using Imaris v9.1.2 (Bitplane/Oxford Instruments) and snapshots segmented by hand in Image J/Fiji. All other images processed and analysed using Fiji. All images, including time lapse snap shots are maximum composites. Median filter applied to all pMad images in Fiji to remove noise. The heatmap was generated using the ROI color coder plugin, part of the BAR collection of ImageJ.

The number of pMad positive cells within the PCV field was calculated by first excluding adjacent LV nuclei by marking the predicted trajectory of the LV–PCV boundary by drawing across from the edge of L4 and L5 on either side of the PCV. All pMad positive nuclei (regardless of intensity of stain) between these lines were then counted. Z projections of median filtered images were used for quantification, using the stacks for reference.

The basal sizes of field cells were analysed using individual slices of stacks in Fiji. Cell outlines on the basal side of cells that showed pMad staining in the nucleus were traced and measured. The most basal slice where the cell outline was clear was used for each cell. Cells at the centre and posterior portion of the PCV were analysed. Cells that run along the edge of the PCV field were designated peripheral cells.

All representative images are representative of at least 3 biological replicates.

Statistics

Statistical analyses were performed using GraphPad Prism software (v.8.3.0, GraphPad). The number for all quantified data is indicated in the figure legends. All P values were calculated using a two-sided Mann-Whitney test and specified in the figure legends and in the corresponding plots.

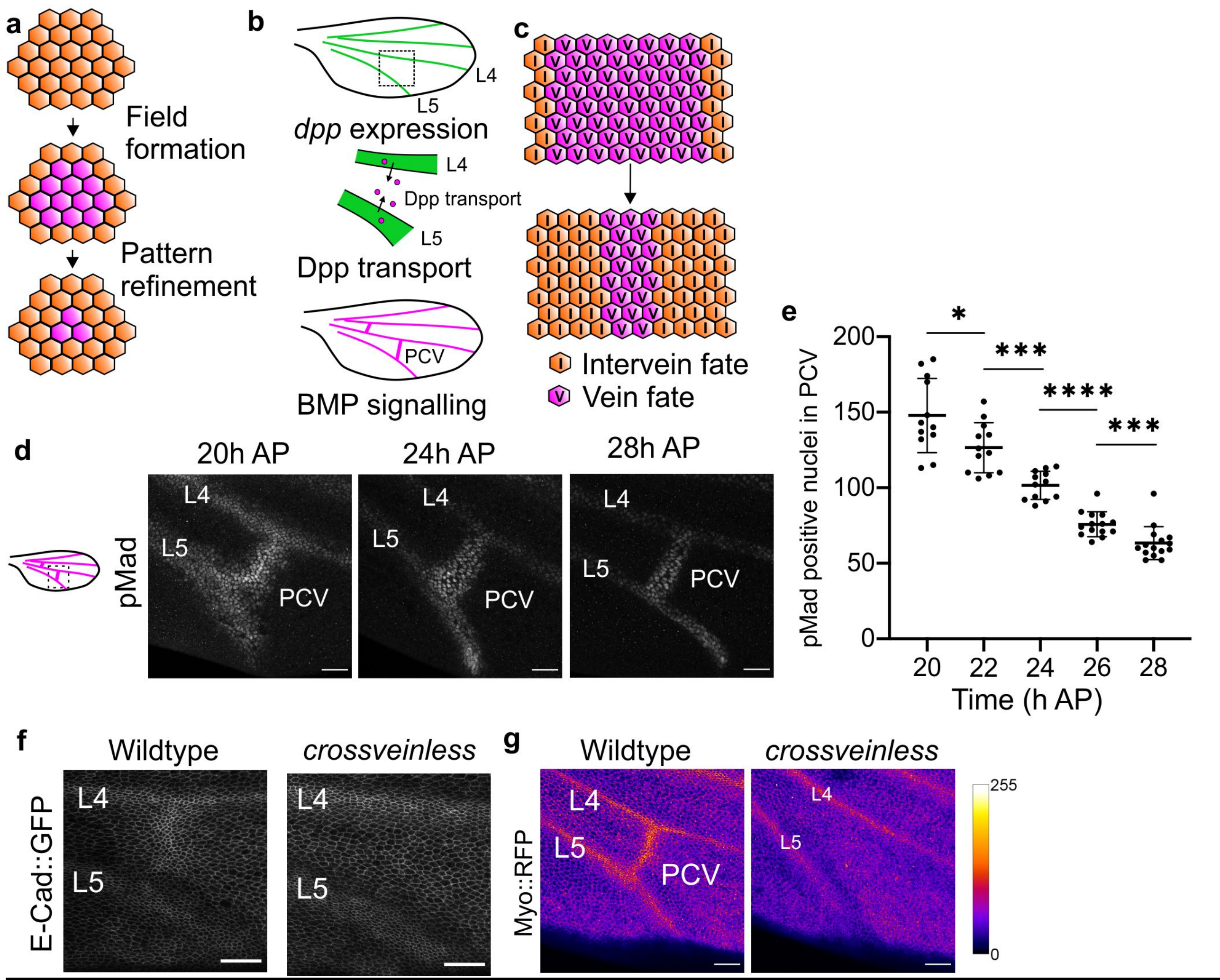

Fig. 1: The PCV field refines during vein patterning and morphogenesis. a, Schematic depicting the refinement of developmental patterns from an initial field to cells committing to a fate. **b,** The expression pattern and signalling pattern of the BMP ligand Dpp in the developing pupal wing. L4, L5, and PCV denote longitudinal veins 4, 5, and posterior crossvein, respectively. Top: *dpp* mRNA (green) is expressed in longitudinal veins but not in crossveins during early pupal stages. Middle: Schematic model of Dpp/BMP ligand transport from the longitudinal veins into PCV. Bottom: BMP signalling (magenta) is detected at all wing vein primordia including longitudinal veins and crossveins. **c,** Schematic depicting the refinement of the BMP signalling pattern in the PCV field. **d,** BMP signalling (shown by pMad) in the PCV field of wildtype *yw* pupal wings at 20 h, 24 h and 28 h AP. Left: Schematic of pupal wing. Approximate position of imaging is shown as a square. Median filter applied. **e,** The number of cells in which BMP

signalling is occurring during the refinement period. Sample sizes are 12 (20 h), 12 (22 h), 12 (24 h), 14 (26 h) and 15 (28 h). $^{*}P = 0.0252$, 22-24h: $^{***}P = 0.0005$, $^{****}P < 0.0001$, 26-28h: $^{***}P = 0.0002$. Data are mean $\pm$ s.d. and were analysed by two-sided Mann-Whitney test. **f,** E-Cadherin::GFP in the PCV region in wildtype (left) and *crossveinless* mutant (right) pupal wings at 24 h AP. Apical cell shapes are highlighted by max composite of E-Cadherin:GFP. **g,** Heatmap of the apical intensity of MyoII::RFP in cells of the PCV region in wildtype (left) and *crossveinless* mutant (right) pupal wings at 24h AP. The distribution of MyoII is shown by max composite of apical sections. Scale bars: 25 μm for **d**, **f** and **g**.

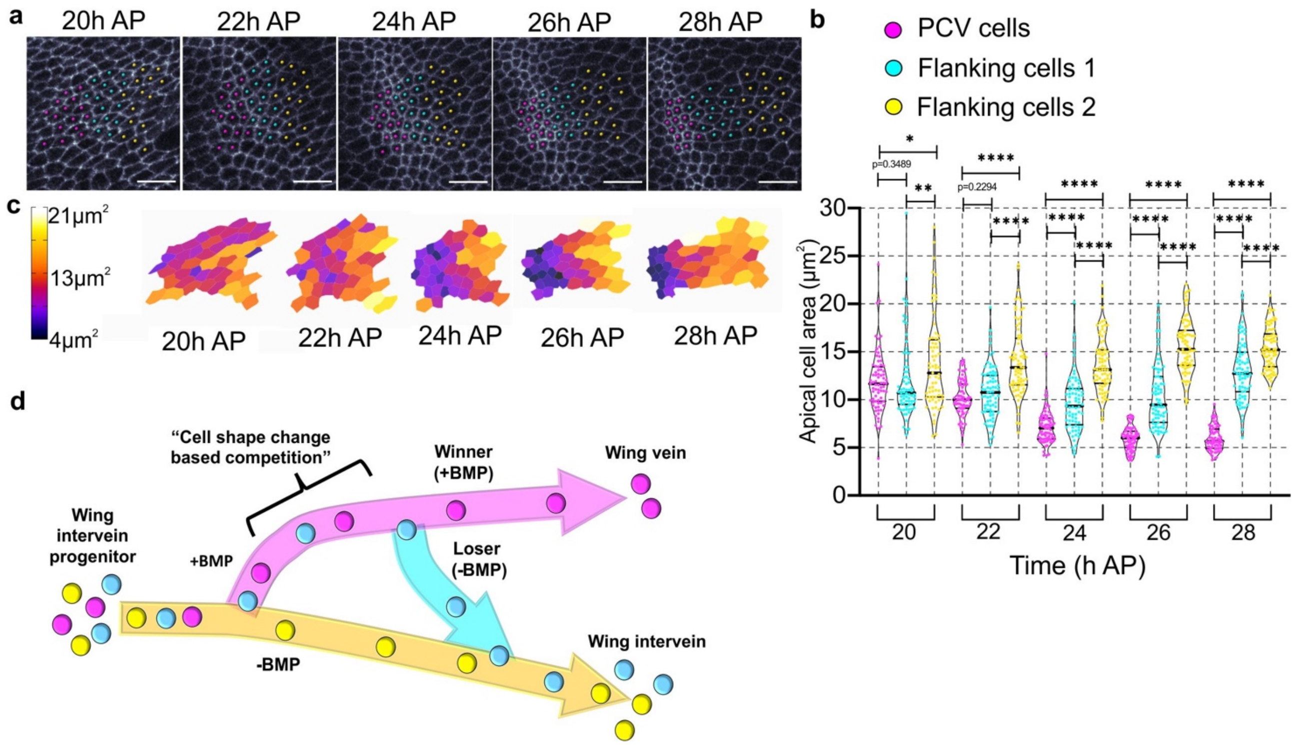

Fig. 2: Changes in cell shape are dynamic and transient during pattern refinement. a, Time-lapse images of E-Cadherin::GFP in the PCV region at 20 h, 22 h, 24 h, 26 h and 28 h AP. Three clusters of cells are marked. Future PCV cells (magenta) show progressive apical constriction. Cells immediately adjacent to future PCV cells (cyan) show transient apical constriction during 22 h and 26 h AP before reverting to an intervein-like structure. Cells further from future PCV cells (yellow) do not show apical constriction. PCV cells are categorised by their shape at 28 h AP and flanking categories by their relative position and shape at 28 h AP. Scale bars: 10 μm. **b,** Apical size of PCV cells and their neighbours during the refinement period. N=75 cells per category (15 cells tracked per category in each wing, for 5 wings). Violin pots show median, and 25th and 75th percentiles. Data from 5 independent time-lapse images. Each data point [PCV cells: magenta, cells adjacent to PCV (Flanking cells 1): cyan, cells further from PCV (Flanking cells 2): yellow] represents one cell. $^*P = 0.0185$, $^{**}P = 0.0071$, $^{****}P < 0.0001$. Data were analysed by two-sided Mann-Whitney test. **c,** Heat map showing the changes in apical area of cells of the PCV field. The heatmap was produced using the ROI color coder plugin, part of the BAR collection of ImageJ. **d,** Schematic of changes in fate path during PCV patterning. Cells that are initially on a vein fate path (cyan) lose

competence during patterning, and move outwith the vein fate path (magenta) into the intervein fate path (yellow). More details about "cell shape change based competition" are described in Fig. 3 and Extended Data Fig. 4.

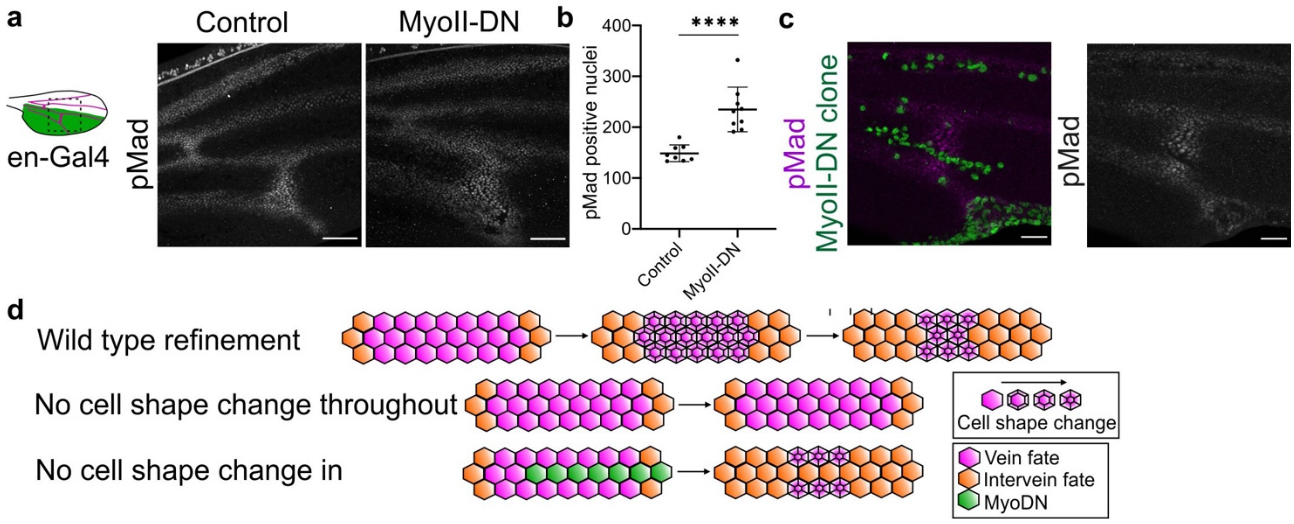

Fig. 3: Loss of MyoII activity has context specific effects on BMP signalling pattern refinement. a, pMad expression in the PCV region in control (middle, *en > mCD8::GFP*) and MyoII attenuated pupal wings (right, *en > MyoII-DN*) at 25 h AP. MyoII-DN was expressed throughout the posterior wing by *en-Gal4* for 10 hours prior to dissection. Approximate position of *en* expression is shown as green in schematic of pupal wing (left). Median filter applied. **b,** Number of cells in which BMP signalling is occurring (and thus are within the PCV field) in the PCV of 25h AP pupal wings. N= 8 (control) and 9 (MyoII-DN). ****$P < 0.0001$. Data are mean $\pm$ s.d. and were analysed by two-sided Mann-Whitney test. **c,** Effects of clonal expression of MyoII-DN within a subset of cells of the PCV field. pMad staining (magenta) MyoII-DN expressing clones (green) at 24 h AP (left), or pMad staining alone (white, right). Median filter applied to pMad staining. Scale bars: 50 μm for **a** and 25 μm for **c**. **d,** Top: Schematic depicting model of wild type pattern refinement whereby loss of cell shape changes from cells at the edge of the PCV field results in their exclusion from the field (by loss of BMP signalling and thus cell fate). Middle: Loss of MyoII activity and cell shape change throughout the PCV blocks refinement**.** Bottom: Loss of MyoII activity in a subset of PCV cells can lead to loss of signal and fate (ectopic refinement).

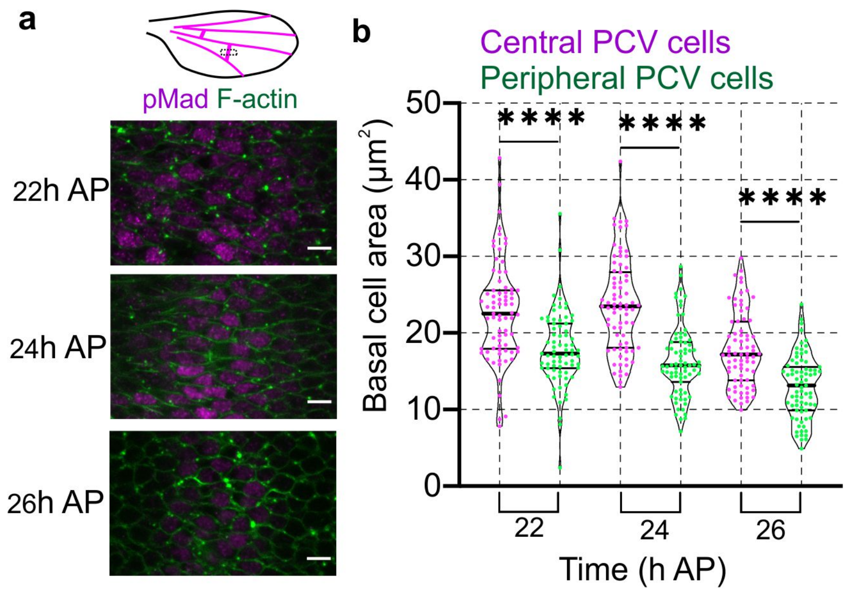

Fig. 4: Central cells in the PCV field that retain vein fate throughout refinement are more basally expanded than their peripheral neighbours. a, Max composites showing basal cell shape of PCV field cells during the refinement period. pMad staining (magenta) and F-actin (green) at 22h AP, 24h AP and 26h AP (left). Top: schematic of pupal wing. Approximate position of imaging is shown as a dotted line. Median filter applied to pMad staining. **b,** Basal cell areas of peripheral cells are smaller than those of central cells during refinement. N = 75 (15 cells per wing, data from 5 wings pooled). Violin pots show median, and 25th and 75th percentiles. Each data point (central PCV cells: magenta, peripheral PCV cells: green) represents one cell. ****$P < 0.0001$. Data were analysed by two-sided Mann-Whitney test.

Extended Data figures

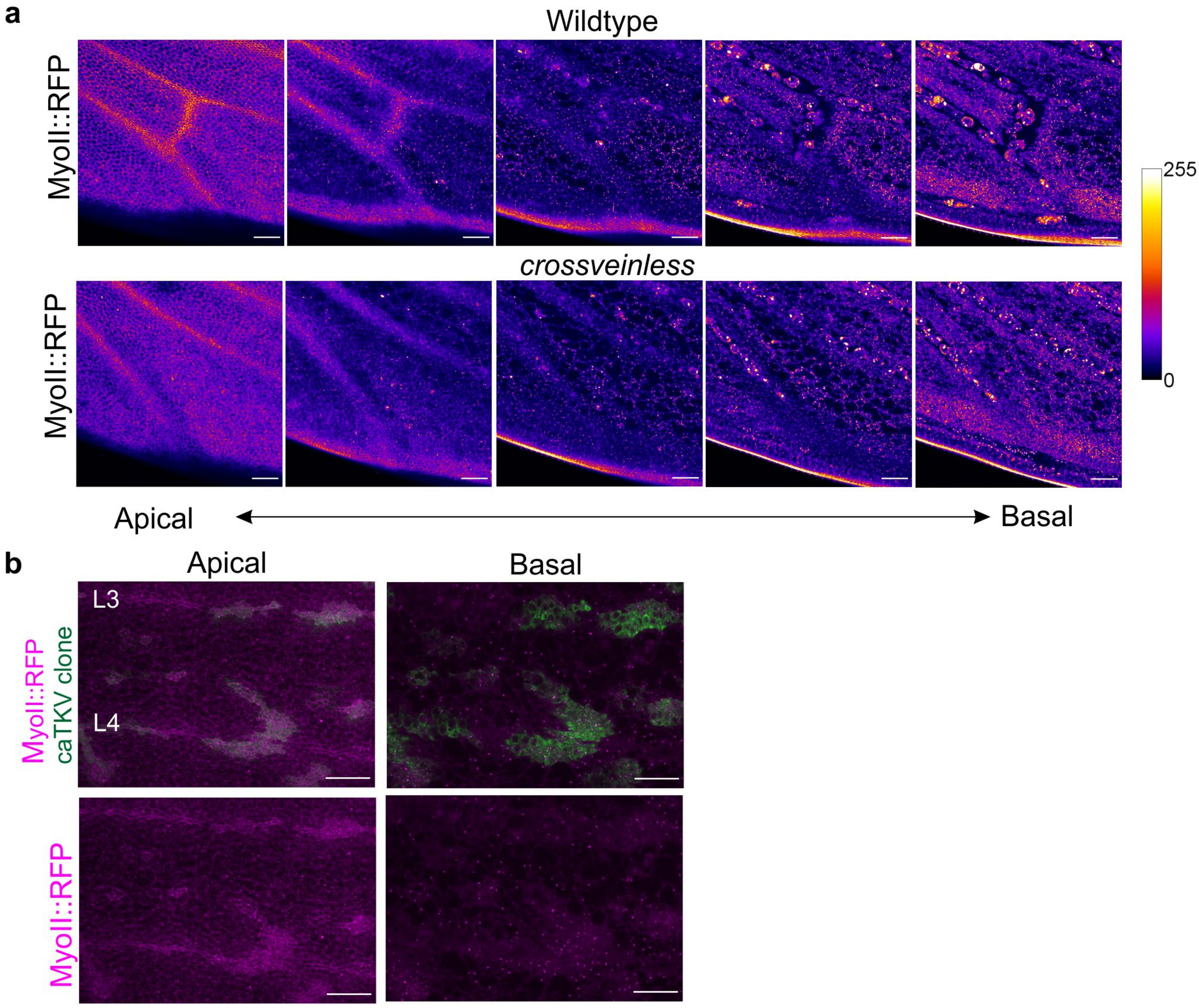

Extended Data Fig. 1: a, MyoII-RFP localisation throughout progressive apical to basal projections of PCV field and intervein cells in wild type and *crossveinless* mutant 24 h AP pupal wings. Max composites of five different sequential sections of the pupal wing along the apicobasal axis. Same tissues shown as in Fig 1g. **b,** Apical and basal max composites showing MyoII-RFP localisation in ectopic clones expressing constitutively active BMP receptor Tkv (25 h AP). Scale bars: 25 μm for **a** and **b**.

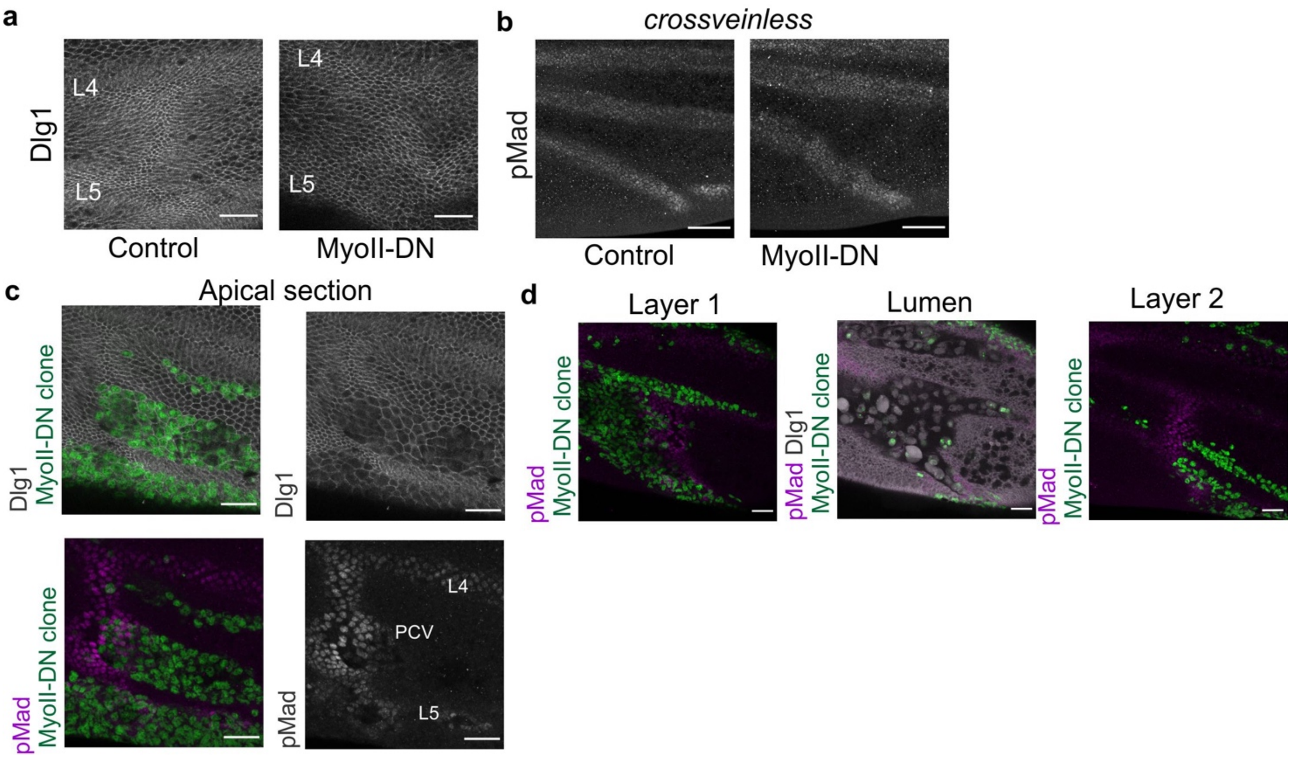

Extended Data Fig. 2: a Apical cell shape (Dlg1) in the PCV region in control (left, *en* > *mCD8::GFP*) and MyoII attenuated pupal wings (right, *en* > *MyoII-DN*) at 25 h AP. From the same dataset as Fig 3a. **b** pMad expression in the PCV region in control (left, *en*) and MyoII attenuated pupal wings (right, *en* > *MyoII-DN*) at 25 h AP in a *crossveinless* background. Median filter applied. **c** Effects of clonal expression of MyoII-DN within a subset of cells of the PCV field on pMad staining (magenta - bottom) and apical cell size (Dlg1 – top) at 25 h AP. MyoII-DN expressing clones are marked by GFP (green). Note that large clones contain cells that both lose and retain the BMP signal despite attenuation of MyoII activity. Median filter applied to pMad staining. **d** Effects of large clones expressing MyoII-DN (left) that disrupt apposition of cell layers and lumen formation (middle), on the other cell layer (right). Median filter applied to pMad staining. Scale bars: 25 µm for **a**, 50 µm for **b,** and 25 µm for **c** and **d**.

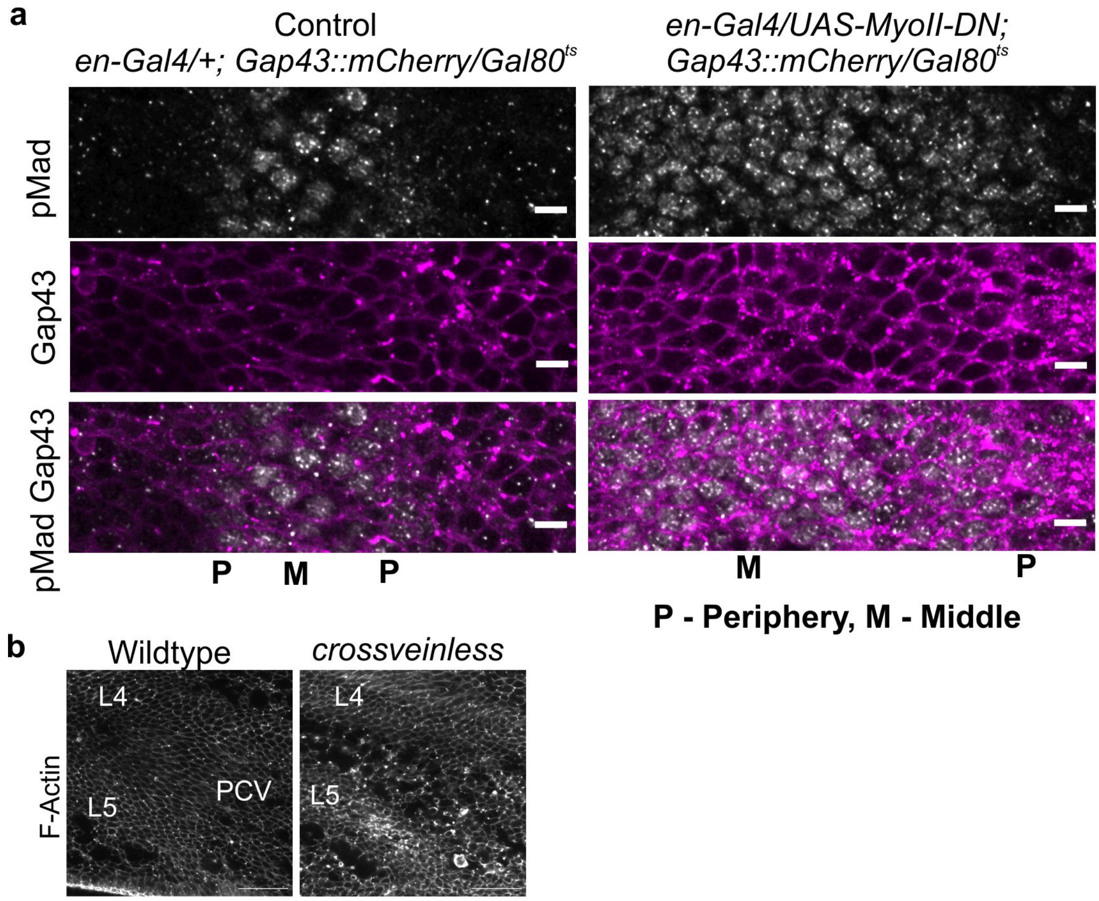

Extended Data Fig. 3: a Basal cell shapes (Gap43 - magenta) in the PCV field (marked by pMad – white) in control (left) and MyoII attenuated pupal wings (right, *en > MyoII-DN*) at 26h AP. Max composite of basal regions of the cells are shown. Middle and periphery of the PCV filed are labelled by M and P. Median filter applied to pMad staining. **b** Basal cell size of PCV field cells in wild type and *crossveinless* mutant 24 h AP wings. Wings are from the same dataset as Fig 1f. Scale bars: 5 µm for **a** and 25 µm for **b**.

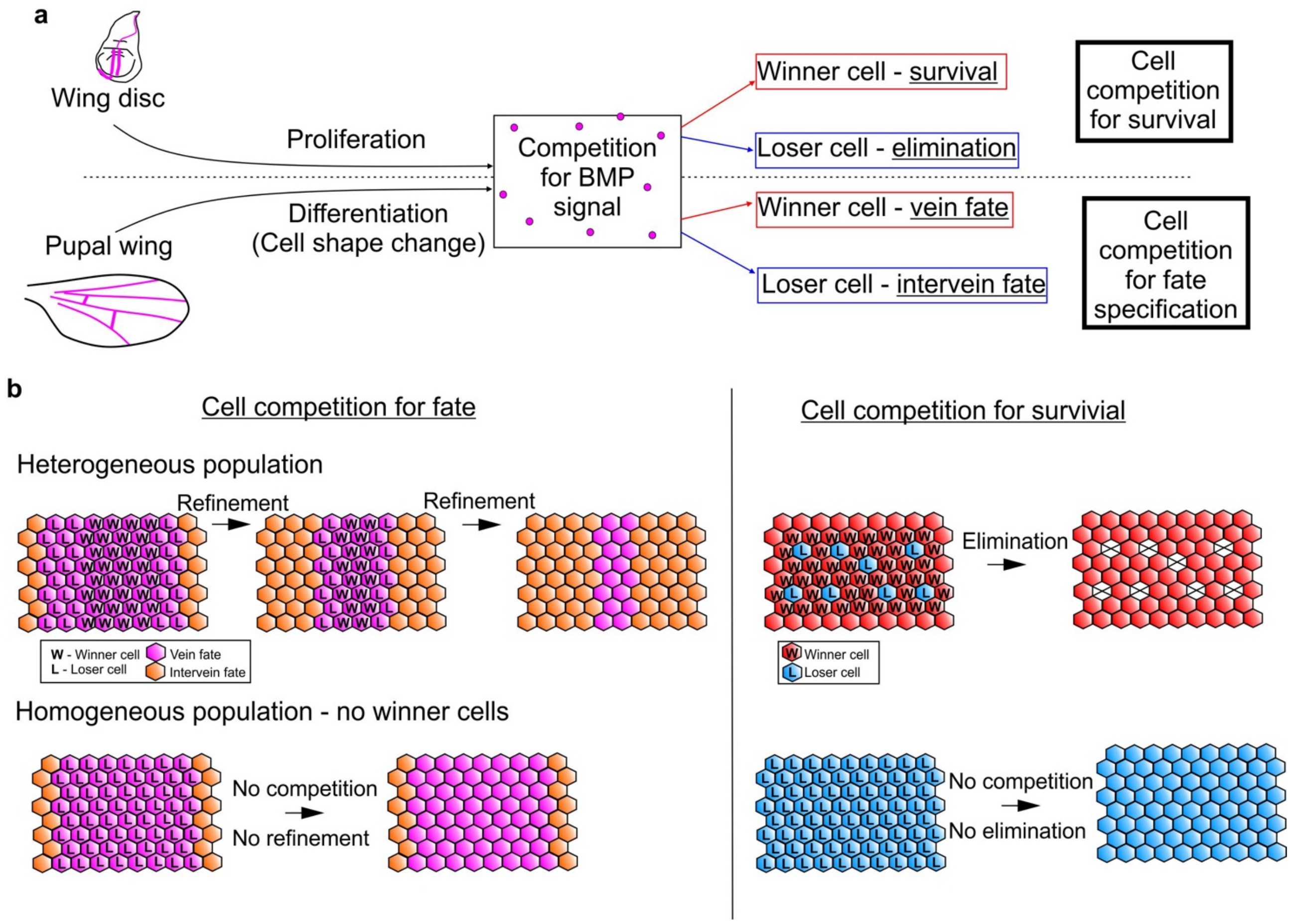

Extended Data Fig. 4: a Schematic showing that competition for the BMP signal in both pupal wing and wing disc can lead to cell competition. In the wing disc the outcome of competition is either elimination or survival, whereas in the pupal wing the choice is either vein or intervein fate. **b** Schematics of cell competition in homogeneous and heterogeneous populations. Top left: Schematic depicting model of wild type pattern refinement whereby loss of cell shape changes from cells at the edge of the PCV field results in their exclusion from the field (by loss of BMP signalling and thus cell fate). Bottom left: Loss of MyoII activity and cell shape change throughout the PCV blocks refinement as no competition occurs. Top right: Classical cell competition in the wing disc, where loser cells are eliminated whilst winner cells survive[23,34]. Bottom right: Loser cells can survive classical cell competition when no winner cells are present[23,34].

Supplementary information

Supplementary Video 1: Time-lapse imaging of E-Cadherin::GFP in the PCV region between 18.5 h and 29.5. h AP. Three clusters of cells are marked. Future PCV cells (magenta) show progressive apical constriction. Cells immediately adjacent to future PCV cells (cyan) show transient apical constriction during 22 h and 26 h AP and revert to intervein-like conformation. Cells distant from PCV cells do not show apical constriction through the time-lapse imaging.

Supplementary Video 2: Time-lapse imaging of E-Cadherin::GFP in the PCV region between 24 h and 28 h AP. Cells marked by magenta and cyan show apical constriction at 24h AP. In contrast, cells only marked by magenta maintain apical constriction at 28h AP, suggesting that cells marked by cyan fail to maintain vein-like morphogenesis.

Supplementary Video 3: Time-lapse imaging of E-Cadherin::GFP in the PCV region between 19h, and 21 h AP prior to apical constriction of future vein cells. Please note that future PCV (magenta) and intervein cells (cyan) are within the same cell lineage at the early PCV morphogenesis.